

## Kinematics of Hyper-Redundant Robot Locomotion with Applications to Grasping

Gregory S. Chirikjian    Joel W. Burdick

School of Engineering and Applied Science  
California Institute of Technology  
Pasadena, CA 91125

### Abstract

*The term 'hyper-redundant' describes robots which are analogous in morphology to snakes, tentacles, or elephant trunks. This paper considers simple schemes for analyzing the kinematics of hyper-redundant robot locomotion over solid terrain. These schemes are based on the concepts of amplitude varying and traveling wave gaits, which are idealized models of inchworm and caterpillar locomotion. The kinematics of these gaits is formulated for hyper-redundant robots of both constant and variable length for locomotion over both flat and irregular terrain. Hyper-redundant locomotion concepts are also applied to a novel grasping and fine manipulation scheme based on a 'grasping wave.'*

### 1. Introduction

The term 'hyper-redundant' is used to describe any robot which has many redundant degrees of freedom. Hyper-redundant robots are analogous in shape and operation to snakes, tentacles, and elephant trunks. This paper considers the locomotion of hyper-redundant robots over solid terrain. We define hyper-redundant locomotion to be the net translation which results from the internally induced bending and/or twisting of a hyper-redundant mechanism. This movement is independent of active wheels or legs.

In nature a wide variety of creatures, such as snakes, worms, and slugs have morphologies which can be considered hyper-redundant. This paper introduces two idealized 'gaits' which mimic the locomotion of inchworms and caterpillars, and shows how these gaits can be implemented in hyper-redundant robots. In this work we consider a 'gait' to be a repetitive sequence of mechanism deformations which cause net motion of the robot. The gaits are demonstrated with planar examples, although the concepts are fully extendible to three dimensional motion. In addition to locomotion, we consider the kinematics of hyper-redundant grasping, and show how the locomotion schemes can be used to implement a novel fine manipulation scheme which is based on a 'grasping wave' concept.

An extensive body of literature has analyzed static walking [6,10], dynamically stable walking and hopping [7,9], and wheeled vehicles [1]. In contrast, the hyper-redundant robot literature has focused primarily on mechanical and system design rather than anal-

ysis [5, and references therein]. Recently, novel actuator technologies have been developed [4] which could be used for hyper-redundant robot locomotion. Qualitative approaches to hyper-redundant mobile robot path planning have also been put forward recently [11]. However, little analysis has been performed for hyper-redundant mobile robots. This paper contributes to the analysis and classification of the kinematics of hyper-redundant locomotion. While some previous hyper-redundant mobile robots have been a hybrid between a snake-like vehicle and a tracked vehicle [5], this paper will consider locomotion without the aid of actuatable wheels, tracks, or legs.

The structure of this paper is as follows. Section 2 presents 'intrinsic' methods for modeling hyper-redundant mobile robot kinematics, and examines two types of nonextensible (fixed-length) hyper-redundant gaits. Section 3 introduces methods for modeling the kinematics of extensible (expandable/contractable) robot gaits. Section 4 introduces the grasping wave concept for the manipulation of objects. Throughout this paper, a variable geometry truss is used to demonstrate the application of these concepts to an actual mechanism. Application to other hyper-redundant morphologies can be found in [2].

### 2. Intrinsic Formulation of Hyper-Redundant Robot Kinematics

We consider only hyper-redundant robots which have a physical structure without macroscopic branches or loops. Robots with fixed length are referred to as *nonextensible*, whereas those which can change length are called *extensible*. This section provides a framework for modeling the kinematics of nonextensible gaits. Section 3 introduces alternate methods for describing extensible gait kinematics.

As in [3, and references therein], it is assumed that the relevant macroscopic geometrical features of both continuous and discrete morphology robots can be captured with a 'backbone curve' which lies along the centerline of the robot. To describe the planar backbone curve a frame defining an  $x_1$ - $x_2$  coordinate system is attached to the base of the robot. The backbone curve is a locus of points in the base frame which have position defined by  $\bar{x}(s,t) = [x_1(s,t), x_2(s,t)]^T$ .  $s$  is the backbone curve arc length measured from the origin of

the base frame, and  $t$  denotes time. All lengths in the plane are scaled to units of the robot length so that  $s \in [0, 1]$ .

With the initial conditions  $\bar{x}(0, t) = \bar{0}$ ,  $\frac{\partial \bar{x}}{\partial s}(0, t) = [0 \ 1]^T$  the backbone curve can be parameterized as follows:

$$x_1(s, t) = \int_0^s \sin \left( \int_0^\sigma \kappa(\mu, t) d\mu \right) d\sigma \quad (1a)$$

$$x_2(s, t) = \int_0^s \cos \left( \int_0^\sigma \kappa(\mu, t) d\mu \right) d\sigma. \quad (1b)$$

The *curvature function*,  $\kappa(s, t) = \pm |\partial^2 \bar{x} / \partial s^2|$ , is defined such that a positive curvature indicates bending in a clockwise sense. The curvature function uniquely defines the planar backbone curve up to rigid body translation and rotation. The clockwise measured angle which the tangent to the backbone curve makes with the tangent to the curve at the back end of the robot is given by

$$\theta(s, t) = \int_0^s \kappa(\sigma, t) d\sigma. \quad (2)$$

The position of all points,  $\bar{r}(s, t)$ , on a planar hyper-redundant robot during locomotion can be specified by:

$$\bar{r}(s, t) = [R(t)]\bar{x}(s, t) + \bar{c}(t). \quad (3)$$

where  $R$  is a  $2 \times 2$  rotation matrix which describes the orientation of the backbone curve base frame relative to a fixed reference frame.  $\bar{c}$  is the  $2 \times 1$  vector from the origin of the reference frame to the origin of the backbone curve base frame. Because of the invariance of the intrinsic formulation with respect to rigid body motion, all geometric features can be formulated in the local backbone curve frame.

The kinematics of nonextensible planar hyper-redundant mechanisms can be reduced to the determination of the spatial and temporal behavior of the curvature function,  $\kappa(s, t)$ . Two classes of nonextensible gaits naturally arise from this intrinsic formulation. In this context, a ‘gait’ is a repetitive sequence of mechanism deformations which cause net motion of the robot. The two categories presented here are by no means the only possible modes of locomotion, but were chosen for their simplicity and wide range of applicability.

The first class of gaits uses an amplitude varying wave which remains stationary with respect to body coordinates. Roughly speaking, an inchworm uses such a wave by extending and contracting its body in a manner in which the ‘hump’ remains in approximately the same location of the body. A second category of gaits, termed traveling wave gaits, which mimics the pedal waves of the slug or the locomotion of a caterpillar is also considered. Complicated forms of locomotion may not fit into either of these categories. The whirling and flagellar movements used for swimming and the sidewinding and concertina modes of snake locomotion are such examples.

The next two subsections consider amplitude varying and traveling wave gaits, with examples to illustrate suitable curvature functions. It is assumed that the robot locomotes over a level surface. Section 2.3 considers locomotion over uneven terrain.

## 2.1 Stationary Wave Amplitude Varying (SWAV) Locomotion

Stationary-wave-amplitude-varying (SWAV) locomotion can be represented with a curvature function of the form

$$\kappa_s(s, t) = \alpha_s(t) \phi_s(s) \quad (4)$$

where  $\phi_s(s)$  is a ‘curvature mode’ and  $\alpha_s(t)$  is the ‘modal participation factor.’ Figure 1 shows time-varying sequences of standing wave locomotion over flat terrain. In this and all figures throughout this paper, the inverse kinematics of the variable geometry truss have been computed using the methods presented in [3]. In SWAV locomotion, forward travel is achieved by varying the the robots curvature by choosing  $\alpha_s(t)$  to be a cyclic function. This method implicitly assumes that the bottom of the mechanism has greater resistance to motion in one direction compared to the other. In practice, this can be achieved with passive wheels which only turn in one direction, or scales which slide during forward motion and exert traction on the ground preventing retrograde motion.

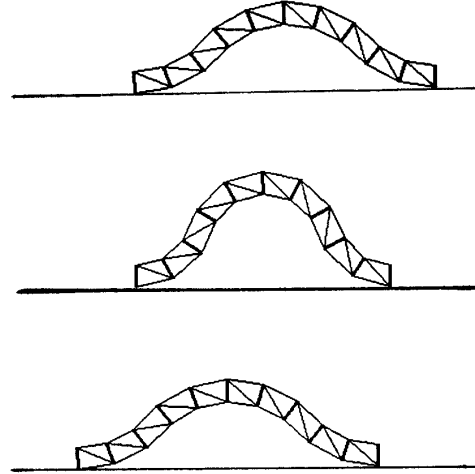


**Figure 1: SWAV Locomotion**

One possible curvature function appropriate to model SWAV locomotion is:

$$\begin{aligned} \kappa(s, t) = & a_1(t)W(s, 0, 1/4) \\ & - a_2(t)W(s, 1/4, 3/4) \\ & + a_3(t)W(s, 3/4, 1) \end{aligned} \quad (5)$$

where the *window function*  $W(s, s_0, s_1)$  is defined to be unity on the interval  $s_0 \leq s < s_1$  and zero otherwise.

The resulting wave is a combination of three circular arcs. The kinematic constraints that both ends of the robot are in contact with, and tangent to, the flat terrain are satisfied by setting:

$$a_1(t) = a_2(t) = a_3(t) = \alpha_s(t) > 0. \quad (6)$$

One possible choice for  $\alpha_s(t)$  is

$$\alpha_s(t) = \alpha_0 + \alpha_1 \cos \omega t. \quad (7)$$

Figure 1 shows the implementation of this curvature function.  $\alpha_0$  and  $\alpha_1$  must obey  $\alpha_{max} > \alpha_0 > \alpha_1 > 0$ . Specifying  $\alpha_{max}$  limits the maximum allowable curvature at any point in the robot. Curvature bounds can arise due to the physical limitations of the robot mechanism or to prevent self-intersection. The constraint  $\alpha_0 > \alpha_1 > 0$  prevents a violation of the kinematic terrain constraints. That is, it prevents the ‘hump’ from penetrating the terrain surface. As  $\alpha_s(t)$  varies, the angle of the tangent at both ends of the inchworm is zero with respect to the  $x_2$  axis,  $\theta(1, t) = \theta(0, t) = 0$ , and from symmetry  $x_1(1, t) = 0$ .

## 2.2 Traveling Wave Amplitude Constant (TWAC) Locomotion

Many terrestrial creatures with hyper-redundant morphologies are capable of sending waves along their bodies for propulsion. In this section we idealize this form of locomotion as a traveling body wave which has constant amplitude. This *traveling-wave-amplitude-constant* (TWAC) form of locomotion can be effected by a curvature function of the form:

$$\kappa_t(s, t) = \phi_t(s - \alpha_t(t)). \quad (8)$$

For example, let

$$\begin{aligned} \kappa_t(s, t) = & a_1 W(s - \alpha_t(t), 0, L/4) \\ & - a_2 W(s - \alpha_t(t), L/4, 3L/4) \\ & + a_3 W(s - \alpha_t(t), 3L/4, L) \end{aligned} \quad (9)$$

where we take the  $\{a_i\}$  to be constants which obey the constraints of Equation (6) (with  $\alpha_s(t)$  taken to be a constant).  $L \ll 1$  is the length of the wave measured along the robot.  $\alpha_t(t)$  could be chosen as

$$\alpha_t(t) = \omega \left[ t - I \left( t, \frac{L+1}{\omega} \right) \right] - L \quad (10)$$

where the function  $I(t, b)$  is defined as

$$I(t, b) = b(\text{int}) \left( \frac{t}{b} \right)$$

for any  $b > 0$ , and  $(\text{int})(x)$  is the greatest integer less than or equal to  $x$ .  $\omega$  is the wave speed. The time varying curvature function in (8) and (9) causes a ‘hump’ of constant magnitude (with the same shape as the

example of Section 2.1) to travel from one end of the torso to the other. Figure 2 shows the motion resulting from this choice of curvature function.

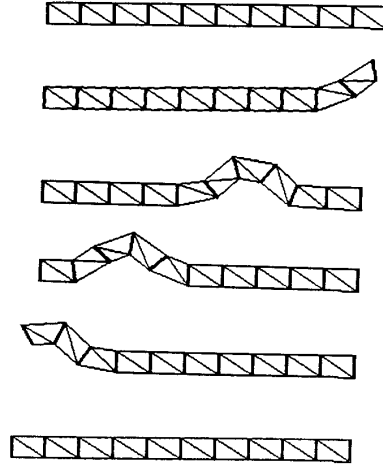


Figure 2: TWAC Locomotion

## 2.3 Locomotion of Nonextensible Robots over Uneven Terrain

The formulation of Sections 2.1 and 2.2 is easily extended to locomotion over curved terrain by modifying the constraints in (6). The waves which result from the curvature functions in (5) and (9) have three degrees of freedom when not constrained by (6), corresponding to the free choices in  $a_1, a_2, a_3$ .

Locomotion over curved terrain requires greater attention to the structure of the curvature function used to define the shape of the locomotion wave. To emphasize this, the notation

$$\kappa(s, t) = \kappa(s, \bar{a}(t), t) \quad (11)$$

is used. This illustrates explicit dependence of the wave shape upon  $\{a_i\}$ .  $\bar{y}(\bar{a}, t)$  is now defined to consist of the relative position and orientation of a frame attached to the robot at  $s = s_1$  (the front of the wave) with respect to a frame attached to the robot at  $s = s_0$  (the back of the wave). The elements of this vector are given explicitly as:

$$y_1(\bar{a}, t) = \int_{s_0}^{s_1} \sin[\theta(s, \bar{a}, t) - \theta(s_0, \bar{a}, t)] ds \quad (12a)$$

$$y_2(\bar{a}, t) = \int_{s_0}^{s_1} \cos[\theta(s, \bar{a}, t) - \theta(s_0, \bar{a}, t)] ds \quad (12b)$$

$$y_3(\bar{a}, t) = \theta(s_1, \bar{a}, t) - \theta(s_0, \bar{a}, t). \quad (12c)$$

We seek to specify the variables  $a_1, a_2, a_3$  such that

$$\bar{y}(\bar{a}, t) = \bar{y}^{des}(t) \quad (13)$$

where  $\bar{y}^{des}(t)$  is the desired trajectory (position and orientation) of the front of the wave with respect to the back of the wave such that the terrain constraints are observed. Unfortunately, unlike the flat terrain case, it may be difficult to solve (13) for  $\bar{a}$ . However, a method analogous to resolved rate schemes can be used. We can express the time rate-of-change of (13) as

$$\dot{\bar{y}}^{des} = \left[ \frac{\partial \bar{y}}{\partial \bar{a}} \right] \dot{\bar{a}} + \frac{\partial \bar{y}}{\partial t} \quad (14)$$

which can be solved for the  $\{\dot{a}_i\}$ . By assuming the robot originates on flat ground, the initial conditions  $\{a_i(0)\}$  can be specified. Integrating at each time step yields a set of  $\{a_i\}$  which defines a wave that tracks the terrain.

This method will not work for all terrains because there is no guarantee that the specified wave shapes will not intersect the terrain, and/or that the Jacobian in Equation (14) remains nonsingular. Algorithms using this technique must check for these situations. The formulation can be amended by using waves with more freedom than the highly constrained form of Equation (5) or (9). The ‘redundancy’ in the wave which is not restricted to a specific form could be resolved by maximizing such quantities as the area between the wave and the terrain.

### 3. Nonintrinsic Formulation of Extensible Locomotion Gaits

This section considers locomotion schemes for gaits which allow for elongation and contraction of the robot. Curves describing the mechanism geometry need not be parameterized by arclength if the nonextensibility constraint is not imposed. Instead, the kinematics of extensible mobile robots is defined relative to the terrain.

Consider a curve which represents a terrain with planar profile. The terrain profile is parameterized in an  $x_1$ - $x_2$  coordinate system by arclength,  $s$ , and every point on this terrain curve is represented by  $\bar{T}(s) = [T_1(s), T_2(s)]^T$  for the interval  $s \in [s_{-\infty}, s_{+\infty}]$ .  $\bar{T}(s)$  is parameterized such that as  $s$  increases, the area to the left of the curve is solid ground, and the robot is on the right hand side. With this parameterization, the outward (upward) unit normal is always of the form:

$$\bar{n}(s) = \begin{bmatrix} T_2'(s) \\ -T_1'(s) \end{bmatrix}. \quad (15)$$

The curve which represents the mobile robot backbone curve, which is now parameterized by *terrain arclength*,  $s$ , is given by:

$$\bar{x}(s, t) = \bar{T}(s) + \rho(s, h(t), t)W(s, s_0(t), s_1(t))\bar{n}(s), \quad (16)$$

for  $s \in [s_b(t), s_f(t)]$ .  $s_b(t)$  is the position of the back of the hyper-redundant robot measured along the terrain, and  $s_f(t)$  is the front. The function  $\rho(s, h(t), t)$

is defined over the domain  $(s, h, t) \in [s_0(t), s_1(t)] \times [h_{min}, h_{max}] \times [t_{init}, t_{final}]$ , and determines the shape of the locomotion wave.  $s_0(t)$  is the distance measured along the terrain from some initial point to the back of the wave, and  $s_1(t)$  is the value of terrain arc length corresponding to the front of the wave. Figure 3 illustrates these quantities.

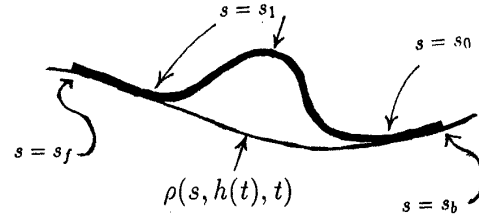


**Figure 3:** Parameters for Extensible Robot Locomotion

The interval  $[h_{min}, h_{max}]$  is defined such that  $h_{min} \leq h(t) \leq h_{max}$  where the function  $h(t)$  determines the amplitude of the extensible locomotion wave. The condition  $0 \leq \rho(s, h_{min}, t)$  for  $s \in [s_0, s_1]$  is imposed to satisfy the constraint of solid terrain, and

$$\rho(s, h_{max}, t) \ll \min_{s \in [s_0, s_1]} \frac{1}{\left| \frac{d^2 \bar{T}}{ds^2} \right|} \quad (17)$$

is required to prevent self intersections of the wave. Appropriate choices for the functions:  $s_b(t), s_0(t), s_1(t)$ , and  $s_f(t)$  further determine the character of the locomotion, e.g., a wave which travels along the robot, one which is stationary with respect to the body, or a combination of the two. Because  $s$  no longer represents the arclength of the robot, but rather is measured along the terrain, the previous definition of robot curvature no longer holds.

The conditions

$$\rho(s_0, h, t) = \rho(s_1, h, t) = 0 \quad (18a)$$

$$\frac{\partial \rho}{\partial s}(s_0, h, t) = \frac{\partial \rho}{\partial s}(s_1, h, t) = 0 \quad (18b)$$

and that  $\rho(s, h, t)$  must be continuously differentiable for all  $(s, h, t) \in [s_0, s_1] \times [h_{min}, h_{max}] \times [t_{init}, t_{final}]$  are needed so that the curve representing the robot is continuously differentiable.

We now consider an example of extensible hyper-redundant robot traveling wave locomotion. An extensible amplitude varying locomotion example can be found in [2]. Figure 4 demonstrates the three phases of extensible traveling wave gaits. In the first phase, which occurs during  $t \in [I(t, t_3), t_1 + I(t, t_3)]$ , the wave starts to traverse the length of the robot, but the whole

wave is not yet in the robot, i.e.,  $s_0(t) < s_b(t) \leq s_1(t)$ . This phase lifts the rear of the robot to initiate a traveling wave. In the second phase, which occurs during the interval  $t \in [t_1 + I(t, t_3), t_2 + I(t, t_3)]$ , the wave is fully contained in the robot, i.e.,  $s_b(t) \leq s_0(t) < s_1(t) \leq s_f(t)$ . In the third phase,  $t \in [t_2 + I(t, t_3), t_3 + I(t, t_3)]$ , the wave exits the front of the robot. For simplicity, in the example shown below we have chosen  $\bar{T}(s) = [-s, 0]^T$ .

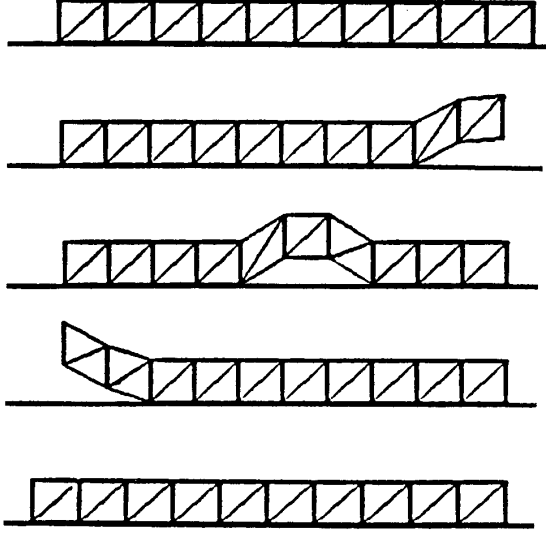


Figure 4: Extensible Traveling Wave Locomotion

By letting  $\omega$  denote wave velocity and  $L_0$  denote the distance the robot progresses with each wave,  $t_1 = L_1/\omega$ ,  $t_2 = 1/\omega$ , and  $t_3 = (1 + L_1)/\omega$ . One possible extensible traveling wave gait can then be defined by:

$$s_1(t) = (1 + L_0)((t - I(t, t_3))\omega + L_0 I(t, t_3))/t_3 \quad (19)$$

and

$$s_0(t) = s_1(t) - L_1 \quad (20)$$

and

$$\rho(s, h, t) = h \sin^2 \left( \frac{\pi(s - s_0(t))}{L_1} \right) \quad (21)$$

where  $h = h_0$  is a chosen constant for this case which determines the height of the ‘hump’. Again, the wave shape, determined by  $\rho(s, h, t)$ , is arbitrary up to the constraints mentioned earlier.  $s_0$  and  $s_1$  are defined so that the wave travels with constant velocity from back to front of the robot, with the process repeating with period  $t_3$ . The positions of both ends of the robot, denoted by terrain arc lengths  $s_b$  and  $s_f$  are chosen to be

$$s_b(t) = (L_0/t_1)(t - I(t, t_3))W(t - I(t, t_3), 0, t_1) + (L_0/t_3)I(t, t_3) + L_0W(t - I(t, t_3), t_1, t_3) \quad (22)$$

and

$$s_f(t) = 1 + (L_0/t_3)I(t, t_3) + \frac{L_0}{t_3 - t_2}(t - t_2 - I(t, t_3))W(t - I(t, t_3), t_2, t_3). \quad (23)$$

This choice for  $s_b$  and  $s_f$  causes the robot to locally stretch and contract as the wave passes. However, no residual stretching or contracting of the robot is passed on between cycles.

The above choices of  $a, \rho, s_0, s_1, s_b, s_f$  constitute one possible gait of the category of traveling wave gaits. One can imagine other gaits which use different wave shapes, combine stationary and traveling waves, or incorporate multiple simultaneous waves.

#### 4. Applications to Grasping

This section applies some of the locomotion ideas to the kinematics of grasping and object reorientations. The hyper-redundant robot, which in this case is fixed to a stationary base, wraps around the solid object to be grasped. In previous work, [8], ‘‘massively redundant’’ tentacle grasping of objects has been considered. Here, we consider the novel combination of a hyper-redundant grasp with a locomotion wave used to reorient the object. In this presentation we consider only the kinematic aspect of grasping and object reorientation.

The proposed grasping and locomotion wave (GALWA) method for manipulating objects consists of the following steps.

- **Shape Initialization:** The hyper-redundant mechanism wraps around the object. The section of the manipulator in contact with the object is termed the *grasp contact segment*.
- **First Phase:** A section of the mechanism which is outside of the grasp contact segment distorts to a wave form. As a result, the object will be displaced by a small amount. This is shown in Figure 5(a).
- **Second Phase:** The wave generated in the first phase travels along the robot toward the distal end without changing the position or orientation of the object over which it passes. This phase (shown in Figure 5(b)) is similar to traveling wave locomotion where the manipulated object is the terrain. When the wave has traveled to the distal end of the manipulator, the grasp contact segment will be longer (by an amount referred to as *stride length* in locomotion terminology).
- **Third Phase:** The manipulator ‘unwraps’ part of the grasp contact segment from the object by straightening a small part of the grasp contact segment as shown in Figure 5(c). This results in a rotation and displacement of the object.

In the case where the object to be manipulated is a cylinder, the displacements resulting from the first and third phases cancel, leaving only a net rotation.

When the third phase is complete, the cycle repeats starting with the first phase. This repetition results in repeated object rotations, the magnitude of which depend on the size of the wave. The cycle shown in Figure 5 can be used as depicted above to cause counter-clockwise rotations. Alternately, the cycle can be reversed to yield clockwise rotations. For arbitrary objects, net translations can also occur from cycle to cycle. These can be compensated for with previously developed methods for hyper-redundant manipulator end-effector placement [3, and references therein].

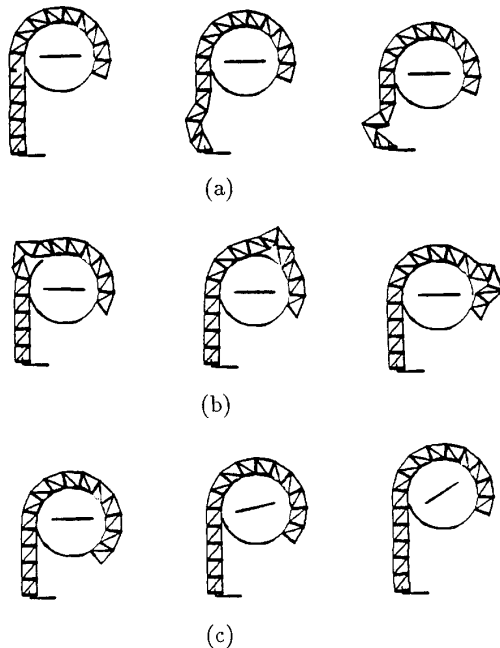


Figure 5: Hyper-Redundant Grasping of a Cylinder

For greater technical detail concerning the curvature functions used to generate Figure 5, see [2].

## 5. Conclusion

This paper modeled the kinematics of hyper-redundant locomotion using methods of the differential geometry of planar curves. Two gait models, which are idealizations of inchworm and caterpillar locomotion, were introduced. These 'Standing Wave Amplitude Varying' and 'Traveling Wave Amplitude Constant' gait models were applied to a variable geometry truss to illustrate their applicability to an actual mechanism. It was shown how these gaits can be used for both extensible and nonextensible robots over flat and curved terrain. In addition, a novel hyper-redundant fine manipulation scheme based on a 'grasping wave' was introduced.

## Acknowledgements

This work was sponsored in part by a NASA Graduate Student Researchers Program fellowship (for the first author), and the Caltech President's Fund, # PF-331.

## 6. References

- [1] Alexander, J.C., Maddocks, J.H., "On the Kinematics of Wheeled Mobile Robots," *International Journal of Robotics Research*, Vol. 8, No. 5, 1989.
- [2] Chirikjian, G.S., Burdick, J.W., "Hyper-Redundant Robotic Locomotion: Locomotion Without Wheels Tracks, or Legs," *Robotics and Mechanical Systems Technical Report No. RMS-89-6*, Dept. of Mechanical Engineering, California Institute of Technology, March 1990.
- [3] Chirikjian, G.S., Burdick, J.W., "Parallel Formulation of the Inverse Kinematics of Modular Hyper-Redundant Manipulators," *1991 IEEE Robotics and Automation Conference*.
- [4] Fukuda, T., Hosokai, H., Kikuchi, I., "Distributed Type of Actuators by Shape Memory Alloy and its Application to Underwater Mobile Robotics Mechanism," *Proceedings of the 1990 IEEE Conference on Robotics and Automation*, Cincinnati, Oh, May. 14-17, pp. 1316-1321, 1990.
- [5] Hirose, S., Morishima, A., "Design and Control of a Mobile Robot with an Articulated Body," *International Journal of Robotics Research*, vol.9., No. 2, 1990, pp.99-114.
- [6] Kumar, V.R., "Motion Planning for Legged Locomotion Systems on Uneven Terrain," Ph.D. dissertation, The Ohio State University, Columbus, Ohio, 1987.
- [7] McGeer, T., "Passive Dynamic Walking," *International Journal of Robotics Research*, Vol. 9, No. 2, 1990.
- [8] Pettinato, J.S., Stephanou, H.E., "Manipulability and Stability of a Tentacle Based Robot Manipulator," *Proceedings of the 1989 IEEE International Conference on Robotics and Automation*, May 15-19, 1989, Scottsdale, AZ, pp. 458-463.
- [9] Raibert, M.H., *Legged Robots That Balance*, The MIT Press, Cambridge Mass., 1986.
- [10] Song, S.M., Waldron, K.J., *Machines That Walk*, The MIT Press, Cambridge, Mass., 1989.
- [11] Stulce, J.R., Burgos, W.E., Dhande, S.G., Reinholtz, C.F., "Conceptual Design of a Multibody Passive-Legged Crawling Vehicle," *Proceedings of the ASME Mechanisms Conference*, Chicago, Il, Sept. 16-19, 1990.